# Relevance of deconsolidation on the porosity of thermoplastic CFRP tubes wound with direct electrical resistance heating

Jonas von Heusinger[1,2], Jonas Naumann[1], Yannis Grohmann[1], Mihai Fetecau, Daniel Stefaniak[1,2], Clemens Dransfeld[2]
1 German Aerospace Center, Ottenbecker Damm 12, 21684 Stade, Germany
2 TU Delft, Mekelweg 5, 2628 CD Delft, Netherlands

## ABSTRACT

Continuous Resistance Heating Technology (CoRe HeaT) uses Joule heating to melt carbon fibre reinforced thermoplastic tapes during automated fibre placement (AFP) or winding, enabling higher deposition rates and improved productivity. Heating of thermoplastic carbon fibre (CF) material causes deconsolidation, voids and release of internal stresses. The extreme heating rates that can be achieved with Joule heating and the challenges with temperature homogeneity that come along, are other factors that can play a role in that regard. The study employs static tests and a CoRe HeaT-assisted winding machine, analysing micrographs with a machine learning-based semantic segmentation model to detect voids. Results show wound tubes have interlaminar voids rather than intralaminar ones, indicating deconsolidation has limited effect on overall porosity. Thus, optimizing compaction at the nip point is crucial for defect-free preforms.

## 1. Introduction

The use of direct resistance heating in automated fibre placement (AFP) and winding processes is a relatively new approach for automated manufacturing of thermoplastic composites. Since Continuous Resistance Heating Technology (CoRe HeaT) allows multiple times faster deposition rates than state of the art in-situ AFP processes, a combined process chain with subsequent post-consolidation for setting the final part properties, can benefit both manufacturing times and part quality, compared to in-situ processes.

For the purpose of understanding the influence of CoRe HeaT on the final part properties and the feasibility of the technology for implementation in industry scale processes, it is necessary to develop a deeper understanding of the single process steps. In order to understand the first step, the preform winding, this paper aims to investigate the deconsolidation when using Joule heating of thermoplastic unidirectional (UD) CF prepreg tapes during the preform winding process. CoRe HeaT is applied both in a static test setup and in a preform winding process. For analysing samples, a machine learning model is trained for semantic segmentation of microscopic images. With this tool, it is possible to estimate quantitative void contents on the basis of 2-dimensional images and to assess their distribution in the cross section. Statically heated tape samples and CoRe HeaT wound preforms are investigated using this method.

# 2. State of the art

## 2.1. CoRe HeaT assisted layup

CoRe HeaT is a heating technology, developed at the Center for Lightweight-Production-Technology (ZLP) of the German Aerospace Center (DLR) for automated layup processes, for dry CF UD tapes or thermoplastic CF prepreg tapes. The technology uses direct resistance heating of the electrically conductive fibres. The aim of manufacturing thermoplastic carbon fibre reinforced polymer (CFRP) components with CoRe HeaT is to perform a rapid layup of preforms with subsequent post-consolidation. With CoRe HeaT-assisted AFP or winding it is possible to increase material throughput significantly to more than $2\,m/s$. By using this process chain, the goal is to both improve part quality and productivity. [1, 2]

It has already been proven, that post-consolidation strategies like stamp-forming or vacuum bag-only consolidation can improve the mechanical properties of preforms that have been manufactured with an AFP process [3, 4].

Highly dynamic intrinsic heating requires suitable thermoplastic CF prepreg materials for being able to achieve good electric contact to the fibres and even heating behaviour in the cross section of the tapes and along the heating zone. High, evenly distributed fibre volume contents and tapes without resin rich surface are favourable for the technology. [5]

In 2024, results of a mechanical testing campaign were published by Grohmann et al. [1]. Thermoplastic UD AFP laminates were produced with CoRe HeaT and then post-consolidated with a hot press, using CF/low-melt polyaryletherketone (LM-PAEK) prepreg tape. The laminates were then compared with mechanical testing to hot pressed UD laminates, manufactured from slitted sheets of pristine mothers roll of the same material. Tensile tests (0° and 90°) as well as interlaminar shear strength tests showed little to no negative impact on mechanical properties for CoRe HeaT laminates. Moreover, it was found, that low power pulses with short pulse lengths are favourable. It was concluded, for future improvement of the technology with the goal of increasing deposition speeds it is useful to switch from AFP to winding, because of less limitations by the kinematics.

## 2.2. Porosity in thermoplastic AFP laminates and wound bodies

Porosity is a common manufacturing defect in AFP laminates and should be minimized in the production process. For meeting aircraft industry requirements the aim is to achieve maximum void contents as low as 1 %. Main sources for voids in AFP parts are intralaminar voids in as-received tape, interlaminar void entrapment during layup and evaporation of volatiles due to introduced heat. [6, 4, 3]

An issue of in-situ AFP processes is the decrease of mechanical properties when the deposition speed is increased, which is why in general in-situ AFP productivity is limited. One

reason for this is that an increase in process velocity correlates with a rise in void content. Void content is limited by several void reduction mechanisms. Pores are compressed by the compaction roller, reducing their size. Moreover, dissolution of gas molecules in the matrix component and diffusion of voids out of the laminate are as well mechanisms of void reduction. [7, 8, 6, 4, 3]

Khan et al. [8] investigated the resulting void contents with microphotography after varying several manufacturing parameters, using a hot gas torch AFP setup. When increasing process velocity from 5 to 9 $m/min$, they observed a rise in void content from $\sim 1.4\,\%$ to $\sim 3.3\,\%$.

For the case of CoRe HeaT winding, as it is used in this paper, the goal is not to achieve perfect part quality during preform production. But in order to perform an efficient post-consolidation, it is necessary that as well the preform is of high quality with low void content. The initial step in preform winding is the intrinsic Joule heating of the CF tape, leading to deconsolidation and an increase in void content due to gas expansion. These voids have to be eliminated as good as possible and additionally, the introduction of voids in the nip point during layup has to be minimized. For CoRe HeaT winding, it is not known yet how the void distribution looks like in preforms and what share interlaminar and intralaminar voids have.

# 3. Methods

In this investigation, firstly a static test setup is used to study the deconsolidation due to Joule heating in carbon fibre tapes, as it is present in the heating zone in the winding process before it touches the mandrel. Moreover, CoRe HeaT winding is used to manufacture tube preforms. These two procedures and the used material are described in this chapter. Last but not least, the extraction of void information from corresponding micrographs based on a semantic segmentation model is introduced.

## 3.1. Thermoplastic CF-prepreg tape

Toray Cetex® TC 1225 T700GC standard modulus carbon UD tape is used for this study. It has a resin content by weight of 34 %, using LM-PAEK semi-crystalline polymer matrix. The slit tape has a nominal width of 6.35 $mm$ and a nominal thickness of 0.14 $mm$. Typical thermal properties of the resin are a melting temperature $T_m = 305\,°C$, a processing temperature window of $340\,°C \leq T_p \leq 385\,°C$, a crystallization temperature $T_c = 263\,°C$ and a glass transition temperature of $T_g = 147\,°C$. [9]

## 3.2. CoRe HeaT Winding

The CoRe HeaT-assisted winding process used in this investigation is shown in Figure 1. Thermoplastic CF tape is transferred to the rotating mandrel with 100 $mm$ diameter made of hard-chrome plated E355 steel, along guiding rollers/pulleys. Two electrodes are necessary for using CoRe HeaT as heating method. The first electrode is located in line with

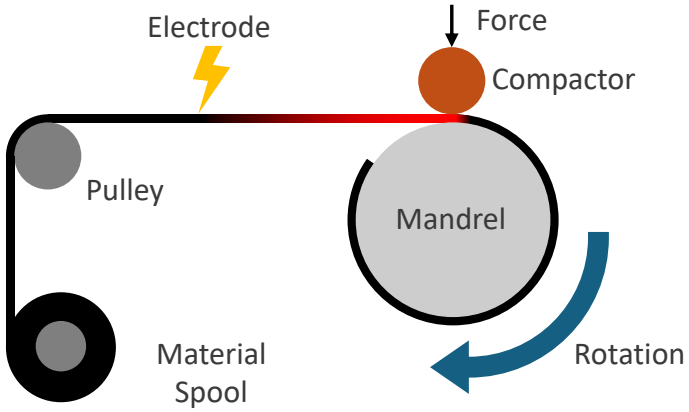


Figure 1: Schematics of a CoRe HeaT winding process.

the tape in front of the mandrel (see Figure 1). When the tape passes the first electrode and voltage is applied, it starts to heat up intrinsically until the compactor presses the tape with force to the mandrel or substrate. The second electrode can be the compactor itself, the metallic mandrel, or a separate electrode, which slides or rolls over the surface of the substrate before or after the nip point. For this investigation, a sliding electrode contacting the substrate after the nip point and another sliding electrode contacting the mandrel are used to close the electric circuit. In the utilized setup and with the given manufacturing parameters, the temperature increase stops after the tape touches the nip point, because heat flux to the compactor and the mandrel/substrate is too high. This might vary when using different electrode configurations, especially at high deposition rates.

As described by Grohmann et al. [1], the control of electric pulses regulates the temperature of the winding process. Pulse power, duration and distance, define the mean heating power.

In this study, a non-conformable copper roller is used as compactor. The compactor is actuated by a pneumatic cylinder. The applied pressure of 1 $bar$ on the cylinder transfers to consolidation pressure of 4.56 $MPa$ at a contact length of $\sim$ 3.8 $mm$ between copper roller and substrate. This was estimated by measuring imprints on pressure sensitive film which was placed between mandrel and compactor while it was being pressed down at the given pneumatic pressure.

Winding speeds of 200 $mm/s$ and 500 $mm/s$ are used for manufacturing tube preforms. Suitable pulse parameters are defined by adjusting them to a level in order to achieve equal layup temperature, which was monitored with a FLIR A615 thermal camera (emission coefficient 0.9). The layup temperature in the nip point cannot be measured during the process, but the surrounding temperatures before and after the nip point, as well as the tack of the material serve as an indicator for adjusting parameters accordingly to achieve roughly comparable processing temperatures $T_p$ as recommended in Section 3.1. The parameter sets that are used for CoRe HeaT winding are listed in Table 1.

The tube manufacturing process starts with fixing the CF tape to the preheated mandrel

Table 1: CoRe HeaT preform winding parameters.

| Tube ID | Tube 01 | Tube 02 |
|---|---|---|
| Layer amount | 8 | 8 |
| Winding speed $[mm/s]$ | 200 | 500 |
| Tape tension $[N]$ | 12 | 12 |
| Mandrel temperature $[°C]$ | 100 | 100 |
| Power $[W]$ | 320-370 | 750 |

with adhesive film. The pneumatic actuators are set active and the process is started. Tape is hoop wound side by side with ideally no gap or overlap. Due to heat, compaction pressure and tape tension, the laid up tape becomes wider, so axial translation per each mandrel rotation has to be adapted accordingly. For the case of $1/4''$ tapes, as it is used in this study, $7\,mm$ of axial translation per mandrel rotation is selected. This results in a winding angle of $\pm 88.72°$. The placement unit moves over the constantly rotating mandrel axially and changes the axial translation direction to start the next layer. In this manner, the process continues until the desired number of layers is reached.

## 3.3. Direct resistance heating deconsolidation testing

In CoRe HeaT-assisted fibre placement or winding processes, Joule heating is being used to heat up carbon fibre tapes intrinsically. For the case of thermoplastic CF prepregs, heating above the melting point $T_m$ of the matrix can lead to deconsolidation of the tape due to expansion of internal voids, evaporation of humidity, and rearranging fibres. In both winding and AFP, the deconsolidated tape gets pressed to the substrate by compaction rollers or the tape tension when it touches the substrate. Thus, it is difficult to monitor deconsolidation in the heating zone in a continuous production process.

Figure 2 shows a test bench for static deconsolidation tests using direct resistance heating. With this setup, the deconsolidation behaviour of tape can be studied with Joule heating

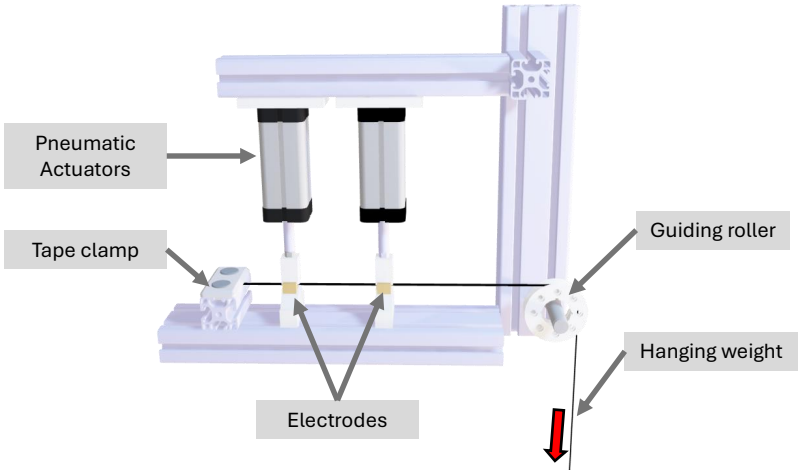


Figure 2: Static direct resistance heating test setup for analysing deconsolidation effects.

Table 2: Static deconsolidation test matrix.

| Run | Tension [$N$] | Heating rate [$°C/ms$] | Temperature [$°C$] | Moisture |
|---|---|---|---|---|
| 0 | 0 | 0 | 0 | Ambient |
| 1 | 10 | $\sim 2$ | $T_m$ | Ambient |
| 2 | 10 | $\sim 2$ | $T_m$ | Water soaked |
| 3 | 10 | $\sim 2$ | $T_m$ | Oven dried |
| 4 | 10 | $\sim 2$ | 120% $T_m$ | Ambient |
| 5 | 100 | $\sim 40$ | 120% $T_m$ | Ambient |
| 6 | 100 | $\sim 40$ | $T_m$ | Ambient |
| 7 | 100 | $\sim 2$ | 120% $T_m$ | Ambient |

and without pressing the tape down with a compactor, as in a continuous process. The tape is set under tension by fixing the tape to the test bench with a clamp on one end and hanging a weight to the tape on the other end, after changing its orientation by the guiding roller. Pneumatic actuators provide sufficient force to achieve a good electrical contact between the electrodes and the tape. Each electrode consists of two copper rods, between which the tape gets clamped. Both electrodes are connected to the CoRe HeaT control unit.

Table 2 shows the parameter sets for deconsolidation testing. The tape tension is controlled by varying the hanging weight. The heating rate depends on the pulse power, the final temperature on the pulse length. By using thermal camera recordings in pre-trials, the pulse duration is adjusted to a level, so that a temperature at melting point of the matrix $T_m = 305\,°C$ is reached, or surpassed to a level of $120\,\% \cdot T_m \approx 366\,°C$. Three moisture conditionings for the tapes are used for testing: ambient, soaked in water for $> 12\,h$ and oven-dried for $> 12\,h$ at $80\,°C$.

The deconsolidated tapes are then cut into five samples of equal length from the part of tape which was located between the two electrode clamps. The samples are embedded and polished for microscopic inspection (see Section 3.4).

## 3.4. Microscopy

After demoulding, four samples are cut from the middle of each tube with a size of approximately $10\,mm \times 20\,mm$. The samples are placed in sample cups in sets of four and embedded with fast-curing 2K epoxy resin. Specimens are then ground and polished with a semi-automatic Buehler EcoMet® 30 table grinder. The polished surface is perpendicular to the fibre orientation, thus, the cross section of the laminate can be examined.

For recording microscopic images of the samples, a digital Keyence VHX-5000 microscope is used with 500× magnification. Mixed lighting settings are configured with coaxial and ring light and no polarisation filter. The settings result in fibres appearing in light grey while the matrix is darker and voids appear almost black (see Figure 3 left).

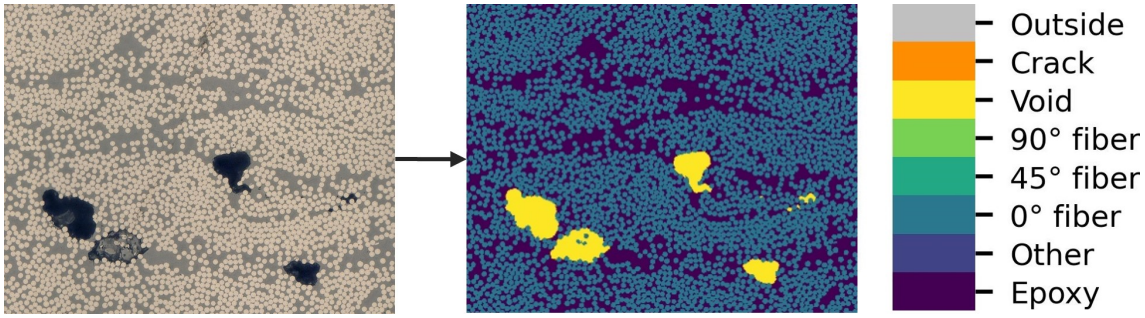


Figure 3: Exemplary micrograph with corresponding training segmentation mask.

## 3.5. Image Segmentation

In Naumann et al. [10], there has already been trained a machine learning-based semantic segmentation model on CFRP micrographs capable to distinguish between *epoxy*, *fibres* of different orientation (*0°*, *45°*, *90°*), *crack*, and *other* (e.g. dirt). The model is based on the widely known convolutional neural network U-Net [11] and the InternImage backbone [12]. Voids barely occur in the dataset used at that time and therefore there has been no corresponding class yet. Due to the demand of this study, it is necessary to increase the capabilities of the model and add a seventh semantic class for *voids*.

To expand the existing, labelled dataset, we annotate two cross section micrographs of a wound and post-consolidated thermoplastic CFRP tube with visible porosity and one of a single-ply tape specimen from deconsolidation testing (see Section 3.3). The outputs of the existing six-class model, where voids are mostly detected, but classified as *other* or *crack*, serve as a good starting point. The following manual corrections are performed using the software LABKIT [13]. For some regions of the single-ply tape specimen, the void labels are only corrected and the remaining ones are set to an index that is ignored during training to reduce the annotation workload. In total, we add 946 patches of size $512 \times 512$ *px*, i.e. around 70 % of the entire, newly labelled data, to the training data split.

This manual correction process includes judging regions of the micrograph as voids manually. By using the described training process, most voids already are assigned to the desired class, but some special cases need to be judged based on best knowledge. In Figure 3, some examples of voids are shown. In the bottom left of the micrograph, there is one void, which does not have the same colour as the others. Apart from the edges it has a lighter grey appearance and three fibres in the middle. In these situations it is judged, that the lighter grey, probably due to reflections because of varying void depths, is still part of the *void* class. The fibres on the other hand, are not counted to the *void* class, since they are clearly distinguishable from the surrounding pixels. Nevertheless, most voids are clearly identifiable due to sharp edges and mostly almost black appearance at given microscopy settings. On the right, much smaller voids can be observed. In the revision process of the training data, it is necessary to be precise on detecting small voids as well, so that the model is trained to detect voids regardless of their size.

The model architecture is not changed except for the required adjustment of adding an

additional output channel for the new class. We train the model from scratch on the complete, expanded dataset for 500 epochs while retaining the previous settings. On the test set of the new, labelled data, the model yields a void pixel recall of 99 % and a void pixel precision of 96 %.

Before applying the model, black colour is assigned to all pixels outside the specimen.To extract the contour of the sample, Fiji's [14] "Wand (Tracing) Tool" is used. The model is specifically trained for segmenting composites. Since embedding resin and composite matrix sometimes can appear very similar, for accurate recognition of the semantic classes and quantitative analysis of data, this step is required to assign these image regions to the label *outside* in the resulting segmentation mask.

### 3.6. Void analysis

After the image segmentation process is finished, the total void content can be calculated by the fraction of the number of pixels that are assigned to the class *void* divided by the number of pixels of all classes, except *outside*.

Each connected component, including diagonal connectivity, in the segmentation mask is considered a void instance. Each of them is characterized by its size (area calculated based on number of pixels and pixel size), its location in the segmentation mask (centroid of all corresponding pixels) as well as its relative vertical position with respect to the specimen/ply boundaries.

## 4. Results

### 4.1. Deconsolidation of UD-tapes after direct resistance heating

Moisture has a large influence on the void content after deconsolidation testing, as it was described in Section 3.3. In Figure 4, the cross section of a pristine tape, as received by the manufacturer, can be seen in comparison to three cross sections of deconsolidated tapes at different moisture conditionings. Moreover, large voids occur near the middle of the tape's thickness.

Large scale pores occur more often in tapes with higher moisture content, as it shows in quantitative data (see Figure 5). While the as-received tape has a void content as low as 0.44 % (Run 0), all other deconsolidated tapes have many times higher void contents and also higher standard deviations as the error bars show. The water soaked sample has the highest void content of all, of 8.82 % and the highest standard deviation, while the dried sample in Run 3 has the lowest standard deviation of all deconsolidated samples.

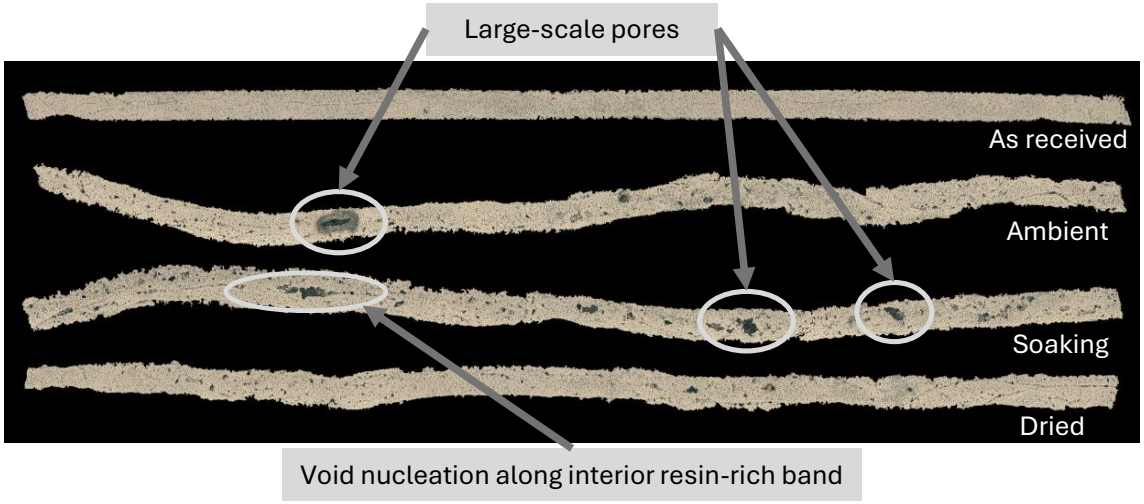


Figure 4: Tape cross section micrographs after deconsolidation (Run 0 - Run 3 according to Table 2).

When comparing Run 1, heated to $T_m$, with Run 4, heated to 120 % $T_m$, the sample which was exposed to the higher temperature has roughly 50 % increased void content. The same tendency applies at higher heating rates of ~ 40 $°C/ms$ as the comparison of Run 5 (heated to 120 % $T_m$) to Run 6 (heated to $T_m$) shows. When the heating rate is increased from ~ 2 $°C/ms$ as in Run 7 to ~ 40 $°C/ms$ as in Run 5, the void content increases as well from 4.67 % to 8.30 %. In Run 7, a ten times higher tape tension was used compared to Run 4, while all other parameters were kept constant. This results in a decrease in void content by 2.64 % to 4.67 %.

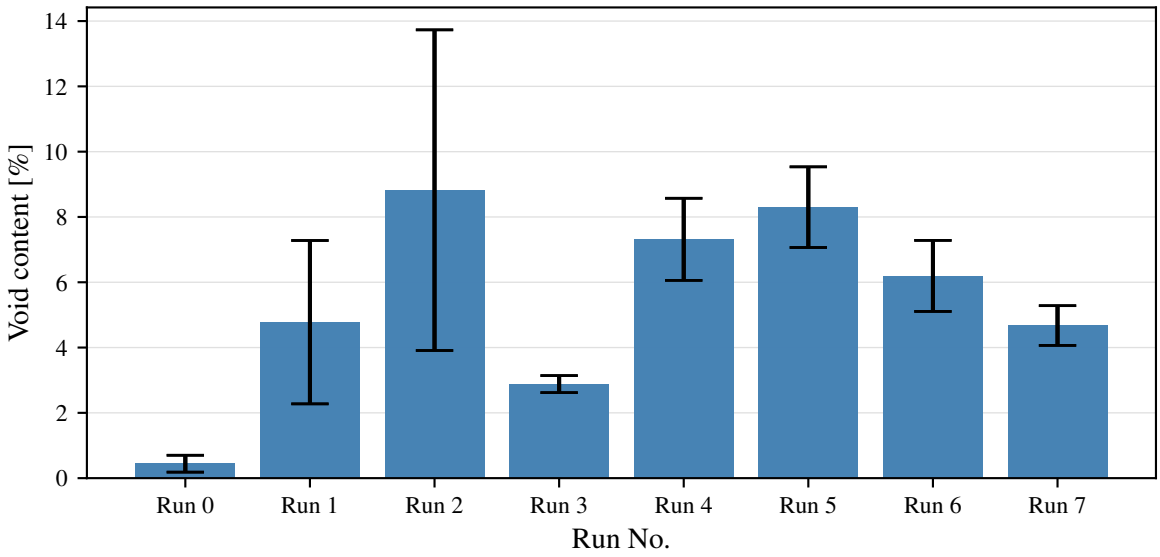


Figure 5: Void content in deconsolidated tapes with testing parameters according to Table 2. Error bars describe the standard deviation of the sample.

## 4.2. Porosity of CoRe HeaT wound tubes

For evaluating preform quality in CoRe HeaT wound tubes, the void distribution of the specimens that were manufactured with the parameters mentioned in Table 1 is analysed. After microscopy samples are investigated with image segmentation as described in Section 3.5, the void instances are characterized according to Section 3.6. The results are visualized in Figure 6, in which the cumulative void content over normalized thickness is derived from the extracted void data. When speaking about cumulative void content, this means that at a given relative thickness of the specimen, the sizes of all voids from the inside of the tube until the given relative thickness are summed up and divided by the total size of the specimen. A thickness of 0 corresponds to the inner surface of the tube, while thickness 1 is the outside tube surface. At thickness 1, the y-value is the total void content of the specimen. Since the wound specimens contain eight layers, the x-axis is split into eight parts by its tick-marks. The shaded area around the graph refers to the standard deviation of all specimens of the run at a specific relative thickness.

Tube 02, which is wound at a higher winding speed of 500 $mm/s$ has a higher total void content of 1.24 %, compared to the Tube 01, which is wound with 200 $mm/s$ winding speed and has a void content of 0.45 %. Both void content values are significantly lower than the void content of deconsolidated tape specimens as the results in Section 4.1 show. Interestingly, both graphs show a stepped, or wavy structure. The steeper inclines of the graphs are correlating with the x-tick-marks.

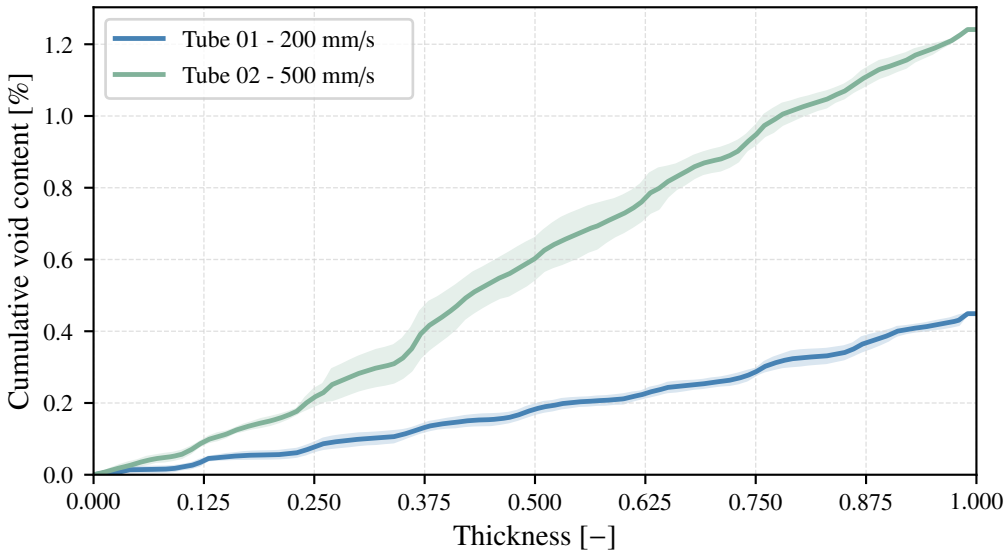


Figure 6: Cumulative void content over thickness in CoRe HeaT wound tubes.

# 5. Discussion

In static deconsolidation experiments, it is shown that direct resistance heating can cause a significant increase in void content in thermoplastic CFRP tapes. All varied parameters, namely moisture content of tape material, tape tension, heating rate, and maximum temperature have an influence on the increase in void content. Overall, higher processing temperatures lead to lower viscosity of the melted matrix, thus, gases in voids can expand easier and fibres rearrange with less restriction by surrounding matrix.

While a clear recommendation can be made for using dried thermoplastic prepregs in CoRe HeaT assisted production processes, it is not that simple for the other parameters because of their interaction with each other in a real production environment. When looking at a dynamic layup process in which the goal is to maximize productivity, the heating rate must be increased accordingly to achieve a processing temperature well over the melting point of the matrix. Even though higher temperatures lead to an increase in void content, lower matrix viscosity facilitates interlaminar bonding under the compactor during automated layup. According to the results, an increase in tape tension leads to less deconsolidation in the heating zone before compaction. It is important to notice, that the exact tape tensions during deconsolidation testing are unknown, since thermal expansion of the tapes combined with the fixation by the pneumatic actuators and the stiffness of the test bench might influence the values. Tape tension is expected to help in lowering void contents during winding as well. Though, an increase in tape tension could as well lead to residual stress in the fibres. Whether residual stress in the final part is desired or not depends strongly on the application, because it might change the part's mechanical properties.

The deconsolidation setup in Figure 2 mimics the heating process between first electrode and nip point of the actual CoRe HeaT winding process (see Figure 1), but with compromises. In the deconsolidation tests, single pulses are configured, that heat up the tape samples to melting point or processing temperature, instead of using pulsed heating as in the winding process. Moreover, the Joule heating of tapes in a static test setup is inherently different from a dynamic setup, because the tape does not pass through the electrodes and does not get compacted by the compactor with the same resulting convectional heat loss. Even though the test setup is not able to emulate the CoRe HeaT winding process perfectly, it is suitable to further investigate the different effects on void development when using resistance heating for processing thermoplastic CFRP tape.

While a significant rise in void content in tapes after deconsolidation testing is observed, the void content in wound tubes is much lower (see Figure 6). This shows, that voids successfully get eliminated during CoRe HeaT winding. An increase in void content is observed when using higher layup speeds, as expected based on literature. Moreover, the standard deviation of the cumulative void content of the wound tubes increases when winding with higher deposition speed, which can be seen in the larger shaded area around the top plot in Figure 6. Due to only two levels of winding speed, no statement can be made to the functional relationship between void content and speed. A maximum void content of 1.24 % was detected in a wound tubes, while there is still big room for

improvement with optimized manufacturing parameters or an improved winding setup.

Interestingly, the distribution of cumulative void content over thickness (see Figure 6) shows a stepped, or wavy shape. Steeper increases of the plot, that refer to a higher accumulation of voids, correlate with the interlaminar regions of the specimens, which, given equal mean layer thickness, should be in the surrounding of the x-axis ticks. Voids rather occur interlaminar than intralaminar, even though significant potential for deconsolidation due to resistance heating is shown in the static deconsolidation experiments. This implies that deconsolidation has less impact on void introduction in the CoRe HeaT winding process compared to interlaminar bonding.

The use of semantic segmentation has proven very useful for understanding deconsolidation mechanisms in single-tape specimens and porosity in wound tubes. Training the model to recognise voids in composite micrographs was very successful and enabled new insights in the void evolution during CoRe HeaT thermoplastic composite production. During image analysis, it was found that due to the much more regular structure of tube micrographs with larger cross sections and a more even surface due to compaction, it was easier to precisely recognise all classes correctly. One reason for this was the tendency to subtle colour variations around voids in deconsolidation micrographs caused by imperfect polishing, that are occasionally misinterpreted as voids. Generally, when analysing specimens with semantic segmentation based on microscopy, it is necessary to keep in mind that it is only possible to estimate the quantitative amount of voids on the basis of 2D images instead of 3D data. For raising the confidence in quantitative results, it can be useful to increase the number of specimens and to select them across a wider area of the part.

# 6. Conclusion and Outlook

Employing direct resistance heating in automated thermoplastic CFRP tape layup, as it is done in CoRe HeaT processes developed at DLR, has the clear opportunity to boost productivity. A two-step workflow, consisting of fast preform winding followed by an optimized post-consolidation of parts, is intended to both increase throughput and part quality.

The goal in this study was to develop a further understanding of the resistance heating-induced deconsolidation of tape and its relevance for the preform porosity. For analysing void content in tapes and preforms a machine learning model was trained on segmenting voids in 2D microscopic images, enabling efficient estimation of void content and assessing the void distribution in the laminate's cross section.

A static test setup is used to mimic the heating zone of a Joule heating assisted production process of thermoplastic CFRP. Maximum temperature, heating rate, tape tension and moisture conditioning are varied. Tapes are heated by resistance heating and micrographs of cross sections of these tapes are analysed with a machine learning-based semantic segmentation. A maximum increase in porosity up to 8.82 % is shown for water-soaked tape, while the pristine tape has a void content of 0.44 %. The void content of oven-

dried tape only rises to 2.88 % with similar heating parameters as for the water-soaked sample. Deconsolidation, a phenomenon which is present in all sorts of automated layup processes for thermoplastic CFRP, is as also present when using direct resistance heating as heating technology. However, heating up thermoplastic composites above their melting point is known to cause deconsolidation and forming of voids [3]. The specific influence of resistance heating on deconsolidation can not be safely differentiated yet, since other heating methods were not used within this study.

Production trials are performed with a CoRe HeaT assisted winding setup, that uses direct pulsed resistance heating. The goal is to evaluate the relevance of deconsolidation in the context of preform manufacturing. The winding setup implements a non-conformable compaction roller at the nip point for supporting interlaminar bonding and void reduction. Preform porosity shows significantly lower values than deconsolidation tests on single tape, while winding speed has a strong impact on void content as expected. Moreover, the analysis of the distribution of voids over laminate thickness shows a stepped shape. Steeper increases of the graphs signal a higher void content in these specific regions. These regions correlate with interlaminar bonding layers of the specimens. Thus, voids tend to be introduced rather due to insufficient interlaminar bonding than due to consolidation. Even though deconsolidation due to Joule heating is a present phenomenon during automated layup (similar as in automated layup processes with other heating technologies) and void content due to deconsolidation can exceed preform porosity by multiple times, it is found, that it is not the most influential factor for preform porosity.

On the basis of these findings, next experiments will address the influence of CoRe HeaT-assisted winding process parameters on the preform porosity. Especially parameters that influence the compaction at the nip point, tape tension and the influence of gaps and overlaps on void content will be of interest. Moreover, the goal is to expand testing to preforms that are produced with winding speeds of $\geq 2\,m/s$. The results of future testing campaigns are aimed to benefit the understanding of the CoRe HeaT winding process. Furthermore, the combined results of this and future investigations will serve as a key component on the journey to prove the productivity and quality benefits of a two stepped process chain of CoRe HeaT preform production and an efficient, subsequent post-consolidation as a novel and smart thermoplastic CFRP manufacturing route.

# Acknowledgements

The authors gratefully thank the German Federal Ministry for Economic Affairs and Energy (BMWE) for supporting the research by funding the project LeiWaCo (03EI3071J). The authors gratefully acknowledge the scientific support and HPC resources provided by the German Aerospace Center (DLR). The HPC system CARA is partially funded by ”Saxon State Ministry for Economic Affairs, Labour, Energy and Climate Action” and ”Federal Ministry of Research, Technology and Space”.

# 7. References


[1] Yannis Grohmann, Jonas von Heusinger, and Daniel Stefaniak. “A STUDY ON AUTOMATED FIBER PLACEMENT OF CF-LM-PAEK USING DIRECT ELECTRICAL RESISTANCE HEATING”. In: *21st European Conference on Composite Materials, ECCM 2024. Proceedings. Vol.5 - Manufacturing*. Proceedings of the 21st European Conference on Composite Materials. July 2024. URL: https://elib.dlr.de/210989/.

[2] J. von Heusinger, Y. Grohmann, and S. Khan. “METHODS FOR THE POST-CONSOLIDATION OF HIGH-SPEED-WOUND THERMOPLASTIC CFRP TUBES”. In: *21st European Conference on Composite Materials*. Vol. 5. July 2024, pp. 698–705. DOI: https://doi.org/10.60691/yj56-np80.

[3] Tjitse K. Slange. “Rapid Manufacturing of Tailored Thermoplastic Composites by Automated Lay-up and Stamp Forming”. PhD thesis. Twente, Netherlands: Universität Twente, 2019. DOI: 10.3990/1.9789036547284.

[4] Jagadeesh K. Narayana Swamy. “Vacuum-bag-only consolidation of fiber-placed thermoplastic composite structures: A study on the void reduction mechanisms for unidirectional C/PEKK materials”. PhD thesis. University of Twente, 2024. ISBN: 978-90-365-6372-7. DOI: 10.3990/1.9789036563734.

[5] Yannis Grohmann. “Continuous Resistance Heating Technology - Risks and Opportunities of a Novel Heating Method”. In: *Proceedings of the 20th European Conference on Composite Materials, ECCM20*. Ed. by Anastasios Vassilopoulo. Proceedings of the 20th European Conference on Composite Materials - Composites Meet Sustainability (Vol 1-6). EPFL Lausanne, Composite Construction Laboratory, 2022, Vol 02 –S. 54. DOI: https://doi.org/10.5075/epfl-298799_978-2-9701614-0-0. URL: https://elib.dlr.de/192910/.

[6] Khaled Yassin and Mehdi Hojjati. “Processing of thermoplastic matrix composites through automated fiber placement and tape laying methods”. In: *Journal of Thermoplastic Composite Materials* 31.12 (Nov. 2017), pp. 1676–1725. DOI: 10.1177/0892705717738305.

[7] Alex Brasington et al. “Automated fiber placement: A review of history, current technologies, and future paths forward”. In: *Composites Part C: Open Access* 6 (Oct. 2021), p. 100182. DOI: 10.1016/j.jcomc.2021.100182.

[8] Muhammad Amir Khan, Peter Mitschang, and Ralf Schledjewski. “Tracing the Void Content Development and Identification of its Effecting Parameters during in Situ Consolidation of Thermoplastic Tape Material”. In: *Polymers and Polymer Composites* 18.1 (Jan. 2010), pp. 1–15. ISSN: 1478-2391. DOI: 10.1177/096739111001800101.

[9] Toray Advanced Composites. *Toray Cetex® TC1225 LMPAEK™ Product Data Sheet*. Accessed: 2026-04-01. Feb. 2026. URL: https://www.toraytac.com/media/3bd72fac-0406-48e4-bfc4-2ffd2398ac0c/a7eCOg/TAC/Documents/Data_sheets/Thermoplastic/UD%20tapes,%20prepregs%20and%20laminates/Toray-Cetex-TC1225_PAEK_PDS.pdf.

[10] Jonas Naumann et al. “ENHANCING COMPOSITE MICROGRAPH ANALYSIS WITH SEMANTIC SEGMENTATION”. In: *SAMPE 2025 Technical Proceedings*. Society for the Advancement of Material and Process Engineering, May 2025. ISBN: 9781934551486. DOI: 10.33599/nasampe/s.25.0098.

[11] Olaf Ronneberger, Philipp Fischer, and Thomas Brox. “U-Net: Convolutional Networks for Biomedical Image Segmentation”. In: *Medical Image Computing and Computer-Assisted Intervention – MICCAI 2015*. Ed. by Nassir Navab et al. Vol. 9351. Lecture Notes in Computer Science. Cham: Springer International Publishing, 2015, pp. 234–241. ISBN: 978-3-319-24573-7. DOI: 10.1007/978-3-319-24574-4_28.

[12] Wenhai Wang et al. “InternImage: Exploring Large-Scale Vision Foundation Models with Deformable Convolutions”. In: *2023 IEEE/CVF Conference on Computer Vision and Pattern Recognition (CVPR)*. IEEE, 2023, pp. 14408–14419. ISBN: 979-8-3503-0129-8. DOI: 10.1109/CVPR52729.2023.01385.

[13] Matthias Arzt et al. “LABKIT: Labeling and Segmentation Toolkit for Big Image Data”. In: *Frontiers in Computer Science* 4 (2022). DOI: 10.3389/fcomp.2022.777728.

[14] Johannes Schindelin et al. “Fiji: an open-source platform for biological-image analysis”. In: *Nature Methods* 9.7 (June 2012), pp. 676–682. ISSN: 1548-7105. DOI: 10.1038/nmeth.2019.